Structural Engineering and Mechanics, Vol. 44, No. 1 (2012) 85-107

DOI: http://dx.doi.org/10.12989/sem.2012.44.1.085

Nonlinear interaction behaviour of infilled frame-isolated footings-soil system subjected to seismic loading

Ramakant Agrawal*[1] and M.S. Hora[2a]

[1]*Department of Civil Engineering,TRUBA Institute of Engineering and Information Technology, Bhopal, India*
[2]*Department of Applied Mechanics, Maulana Azad National Institute of Technology, Bhopal, India*

(Received March 3, 2012, Revised August 8, 2012, Accepted September 24, 2012)

Abstract. The building frame and its foundation along with the soil on which it rests, together constitute a complete structural system. In the conventional analysis, a structure is analysed as an independent frame assuming unyielding supports and the interactive response of soil-foundation is disregarded. This kind of analysis does not provide realistic behaviour and sometimes may cause failure of the structure. Also, the conventional analysis considers infill wall as non-structural elements and ignores its interaction with the bounding frame. In fact, the infill wall provides lateral stiffness and thus plays vital role in resisting the seismic forces. Thus, it is essential to consider its effect especially in case of high rise buildings. In the present research work the building frame, infill wall, isolated column footings (open foundation) and soil mass are considered to act as a single integral compatible structural unit to predict the nonlinear interaction behaviour of the composite system under seismic forces. The coupled isoparametric finite-infinite elements have been used for modelling of the interaction system. The material of the frame, infill and column footings has been assumed to follow perfectly linear elastic relationship whereas the well known hyperbolic soil model is used to account for the nonlinearity of the soil mass.

Keywords: finite element method; infilled frame; infill wall; nonlinear analysis; hyperbolic soil model; differential settlement; decay pattern; infinite elements; truncation boundary

1. Introduction

In common structural design practice the foundation loads from structure analysis are obtained without considering allowance for soil settlements. The foundation settlements are estimated assuming a perfectly flexible structure. Such an analysis of frame-foundation-soil system may often lead to unrealistic solution and sometimes, it may lead to failure as the stiffness of the structure can restrain the displacements of the foundations and even small differential settlements of the foundations may also alter the forces of the structural members significantly. Thus, it is necessary to consider building frame, foundation and soil mass as single integral compatible structural unit for realistic analysis of the interaction system.

Various investigators have reported the beneficial aspects of infilled masonry in providing load-

*Corresponding author, Ph.D., E-mail: rk_agrawal006@rediffmail.com
[a]Ph.D.

sharing system in concrete and steel frame structures especially in resisting lateral loading caused due to seismic effects or wind loading etc. The earthquake motion affects the interaction behaviour significantly as it produces lateral thrust on the structures. Many investigations have been made to predict the structural behavior of infilled frame under vertical, lateral and cyclic loading. It is established that the composite action of the infill and the frame could be idealized by replacing the infill with an equivalent diagonal strut. Thus, more realistic structural behaviour can be predicted by considering the interaction between infilled frame, isolated column footings and nonlinear soil media which undergoes differential settlements.

2. Literature review

Desai *et al*. (1982) presented a finite element procedure for the general problem of three-dimensional soil-structure interaction involving non-linearity caused by material behaviour, geometrical changes and interface behaviour. The formulation presented is based on the updated Lagrangian approach with appropriate provision for constitutive laws.

Desai *et al*. (1985) developed hybrid finite element procedure for nonlinear elastic and elasto-plastic soil-structure interaction analysis including simulation of construction sequences.

Aljanabi *et al*. (1990) studied the interaction of plane frames with an elastic foundation of the Winkler's type, having normal and shear moduli of sub-grade reactions. An exact stiffness matrix for a beam element on an elastic foundation having only a normal modulus of sub-grade reaction was modified to include the shear modulus of sub-grade reaction of the foundation as well as the axial force in the beam. The results indicated that bending moments might be considerably affected according to the type of frame and loading.

Viladkar *et al*. (1991) used coupled finite-infinite elements for physical modelling of superstructure-soil interaction system and considered the soil mass to behave nonlinearly. It provided improved modelling of soil-structure interaction problem. The approach is logical, more rational and easy for computer implementation.

Noorzaei *et al*. (1994) presented the influence of strain hardening on soil-structure interaction analysis of a plane frame-combined footing-soil system taking into account the elasto-plastic behaviour of the compressible sub-soil and its strain hardening characteristics.

Fardis and Panagiostakos (1997) studied the effects of masonry infill on the global seismic response of reinforced concrete structure by numerical analysis. It was found that the response spectra of elastic SDOF frames with nonlinear infill show that despite their apparent stiffening effect on the system infill reduce spectral displacements and forces mainly through their high damping in the first large post-cracking excursion. It was concluded that the effects of soft-ground storey are not so important for seismic motion at the design intensity, but these effects may be very large at higher motion intensities.

Mandal *et al*. (1998) proposed a computational iterative scheme for studying the effect of soil-structure interaction on axial force, column moments. The results obtained from the computational scheme were validated from experimental study. A small-scale two-storeyed two-bay frame made of Perspex was analysed. The frame was placed on a kaolin bed with adequate arrangement of drainage. The proposed computational scheme could be used to predict increase in axial force and moments in structural members due to the effect of soil- structure interaction.

Manos *et al*. (2000) studied the influence of masonry infill on the earthquake response of multi-storey reinforced concrete structure. In this study, two test sequences were presented: first a 7-storey 2-D plane frame model on 1/12.5 scale, was tested at the Earthquake Simulator of Aristotale University whereas the second, a much larger 3 model, of a 6-storey frame, on 1/3 scaled, (3-D frame) model located at the European Test Site at Volfi. Both structures were examined with and without masonry infill.

Stavridis (2002) presented the simplified analysis of layered soil-structure interaction. The stratified soil was represented with a linear elastic half space model with specific geometrical and elastic properties for its layers.

Asteris (2003) investigated the influence of the masonry infill panel opening in the reduction of the infilled frames stiffness. A parametric study has been carried out using as parameters the position and the percentage of the masonry infill panel opening for the case of one-story one-bay infilled frame. The investigation has been extended to the case of multistory, fully or partially infilled frames. In particular, the redistribution of action effects of infilled frames under lateral loads has been studied. It is shown that the redistribution of shear force is critically influenced by the presence and continuity of infill panels. The presence of infills leads, in general, to decreased shear forces on the frame columns. However, in the case of an infilled frame with a soft ground story, the shear forces acting on columns are considerably higher than those obtained from the analysis of the bare frame.

Doo and Yun (2003) presented time domain method for soil-structure interaction analysis under seismic excitation. The method is based on the finite element formulation incorporating infinite elements for the far field soil region. The earthquake response analyses were carried out on a multilayered half-space and tunnel embedded in a layered half space with the assumption of the linearity of the near and far field soil region.

Junvi *et al*. (2003) presented a coupling procedure of finite element (FE) and scaled boundary finite element (SBFE) for three-dimensional dynamic analysis of unbounded soil-structure interaction in the time domain.

Lehman *et al*. (2004) carried out a complete analysis of soil-structure interaction problems which includes a modelling of near surrounding of the building (near field) and a special description of the wave propagation process in large distance (far field).

Moghaddam (2004) introduced a new analytical approach for the evaluation of shear strength and cracking pattern of masonry infill panels. This approach is based on minimizing the factor of safety with reference to the failure surfaces and can also be used to determine the shear strength parameters and the modulus of elasticity of brickwork material. He presented the results of both experimental and analytical investigations on repaired and strengthened brick infilled steel frames. Two main repair techniques were examined in which the corner material is replaced with concrete or a concrete cover is placed on the panel. Both experiment and analysis have confirmed the efficiency and adequacy of these techniques.

Hora and Patel (2005) proposed computational methodology for non-linear soil-structure interaction analysis of infilled building frames to assess more realistic and accurate structural behaviour. The results revealed the significance of the nonlinearity of soil mass on the interaction behaviour of infilled building frames.

Kaushik *et al*. (2006) reviewed and compared analysis and design provisions related to MI-RC frames (Masonry infill-reinforced concrete frames), in seismic design codes of 16 countries and identifies important issues that should be addressed by a typical model code.

Singh and Das (2006) analyzed a two-dimensional reinforced concrete building frame to investigate the behaviour of multi-storeyed building frames with and without soil-structure interaction effect adopting spring analogy method in which appropriate spring constants were introduced at the foundation level replacing the fixed foundation condition.

Abate *et al*. (2007) investigated the dynamic seismic response of a fire station building structure considering soil plasticity and soil-foundation plastic hinges. The sliding at the soil foundation interface, uplifting of the foundation from the soil and mobilization of bearing capacity failure were taken into account. Orakdoen and Girgin (2008) presented a case study for the performance evaluations of 3-D building frame strengthen by additional shear walls by considering the foundation settlement effects. The nonlinear soil-structure interaction analysis of the building frame-soil system was presented using FEMA-440.

Asteris (2008) proposed a realistic criterion to describe the frame-infill separation in order to better simulate the complicated behaviour of infilled frames under lateral loads. The basic characteristic of the analysis was that the contact lengths between the infill and the contact stresses are estimated as an integral part of the solution. Using this analysis, the response of a single-bay single storey masonry infilled RC frame, under a lateral load at the beam level, was investigated.

Mohebkhah *et al*. (2008) proposed a two-dimensional numerical model using the specialized discrete element method (DEM) software UDEC (2004) developed for the nonlinear static analysis of masonry-infilled steel frames with openings subjected to in-plane monotonic loading. In this model, large displacements and rotations between masonry blocks are taken into account. It was found that the model can be used confidently to predict collapse load, joint cracking patterns and explore the possible failure modes of masonry-infilled steel frames with a given location for openings and relative area. Results from the numerical modeling and previous experimental studies found in the literature are compared which indicate a good correlation between them. Furthermore, a nonlinear analysis was performed to investigate the effect of door frame on lateral load capacity and stiffness of infilled frames with a central opening.

Puglisi *et al*. (2009) proposed a new model to investigate the behaviour of masonry infilled frames. The model is based on the theory of plasticity and the concept of an equivalent strut. The well known nonlinear hyperbolic model was adopted to account for the nonlinear stress-strain behaviour of the soil mass. The results revealed the significance of the nonlinearity of soil mass on the interactive response of the structure.

Puglisi *et al*. (2009) proposed a model to investigate the behaviour of infill panels in framed structures. The proposed model is based on the equivalent strut model, the concept of a plastic concentrator and damage mechanism. An experimental study of the behaviour of masonry specimens under compression forces was presented. These results thus obtained were used for the development of the constitutive law for the equivalent strut bars.

Chore *et al*. (2010) examined the effect of soil-structure interaction on a single-storey, two-bay space frame resting on a pile group embedded in the cohesive soil (clay) with flexible cap. A model is worked out separately for the pile foundation by using the beam elements, plate elements and spring elements to model the pile, pile cap and soil respectively. Negulescu and Foerster (2010) proposed a simplified methodology to evaluate the mechanical performances of buildings exposed to landslide hazard, by using procedure based on Capacity Spectrum Method. It was proposed to assess vulnerability for simple one bay-one storey reinforced concrete frame structures subjected to differential settlements, using 2-D parametric nonlinear static time-history analyses.

Yousuf and Bagchi (2010) presented the performance of a 20-story steel moment resisting steel frame, designed for western part of Canada. Simulated and actual (scaled) ground motion records were used to evaluate the dynamic response. The direct displacement-based design method is found to be more suitable for carrying out the performance-based design of a building.

Asteris *et al*. (2011) presented a general review of the different macro models used for the analysis of infilled frames. A number of distinct approaches in the field of analysis of infilled frames since the mid-1950s have yielded several analytical models. These studies stressed that the numerical simulation of infilled frames is difficult and generally unreliable because of the very large number of parameters to be taken into account and the magnitude of the uncertainties associated with most of them. The advantages and disadvantages of each macro model were pointed out, and practical recommendations for the implementation of the different models were indicated.

Chrysostomou and Asteris (2012) documented the important contribution of infill walls in the resistance of earthquake loads along with a presentation of the behavior modes of the infill and the bounding frame. Equations for quantifying the in-plane stiffness, strength and deformation capacity of infills are given as well as simplified methods for predicting the in-plane failure mode of mainly solid panels. A parametric study is performed to compare these methods and check them against experimental results whenever this was possible. Based on the above material, recommendations are made for the in-plane material properties, failure modes, strength and stiffness as well as deformation characteristics of infilled frames.

In the present study, a two-bay ten-storey reinforced concrete brick infilled building frame resting on isolated column footing (open foundation) and homogeneous soil system is considered to investigate the nonlinear interaction behaviour under seismic forces.

3. Finite element modeling

The interaction analysis requires an efficient computational scheme. The finite element method has been used as the numerical technique for the solution of the problem. The analysis requires various types of isoparametric elements to idealise the interaction system. The floor beams, columns and footing are discretized using three node beam bending element with three degrees of freedom per node (u, v, φ). The infill wall has been discretized with eight node isoparametric plane stress elements with two degrees of freedom per node (u, v). The unbounded domain of the soil mass has been represented by eight noded isoparametric plane strain finite elements elements coupled with six noded infinite elements ($1/r$ type of decay pattern) with two degrees of freedom per node (u, v). A doubly infinite element ($1/r$ type of decay pattern) with two degrees of freedom per node (u, v) is used as a corner element in the finite-infinite element mesh. A finite element based computer programme has been developed in FORTRAN-90 for nonlinear interaction analysis of frame-foundation-soil system.

4. Nonlinear hyperbolic soil model

The stiffness of the reinforced concrete frame is much higher in comparison to that of soil mass. Therefore, in the present investigations, material nonlinearity of the soil mass is considered while the reinforced concrete is assumed to follow the linear stress-strain relationship. The non-linearity of soil mass is represented using the hyperbolic model proposed by Kondner and Zelasko (1963). The model is used in the literature by Duncan and Chang (1970) for nonlinear stress analysis of soil.

The tangent modulus (E_T), of the soil mass at any deviatoric stress level is evaluated as

$$E_T = \left[1 - \frac{R_f(1-\sin\phi)(\sigma_1-\sigma_3)}{2(c\cos\phi + \sigma_3\sin\phi)}\right]^2 E_i \tag{1}$$

Where,
$$E_i = KP_a\left(\frac{\sigma_3}{P_a}\right)^n \tag{2}$$

Various parameters representing the non-linearity of soil mass are:

E_i = Initial tangent modulus
c = Cohesion
P_a = Atmospheric pressure
σ_1, σ_3 = Major and the minor principal stresses
ϕ = Angle of internal friction
K = Modulus number
n = Exponent determining the variation of initial tangent modulus E_i, with confining pressure σ_3.

R_f = Failure ratio = $\dfrac{(\sigma_1-\sigma_3)_f}{(\sigma_1-\sigma_3)_{ult}}$

Where,
$(\sigma_1-\sigma_3)_f$ = Compressive strength
$(\sigma_1-\sigma_3)_{ult}$ = Asymptotic value of deviatoric stress

Poisson's ratio has been kept constant in the analysis. This hyperbolic model has been incorporated into the computer code developed for nonlinear analysis.

6. Nonlinear analysis

6.1 Problem under investigation

A two-bay ten-storey infilled frame of height 30 m and bay width 4.5 m each with isolated column footings (open foundation) is considered to investigate the nonlinear interaction behaviour. The problem under investigation is discretized using coupled finite-infinite elements. Fig. 1 shows the finite element idealization of the problem.

It is assumed that a perfect rigid connection exists between the infill and the bounding frame and there is no slip and sliding takes place between them. The geometrical and material properties of the frame and the soil are provided in Table 1.

In the present investigations, the nonlinear interaction analysis (NLIA) of two-bay ten-storey plane frame-homogeneous soil system (PF-HS) and infilled frame-homogeneous soil system (INF-HS) has been carried out considering the frame and the infill to follow linear stress-strain relationship whereas the subsoil to follow nonlinear stress-strain relationship. The building frame has a bay width of 4.5 m and total height of 30.0 m. The floor beams and plinth beams carry total U.D.L. of 40 kN/m which includes dead load and live load.

The seismic loads are evaluated considering the structure located in seismic zone V of India and

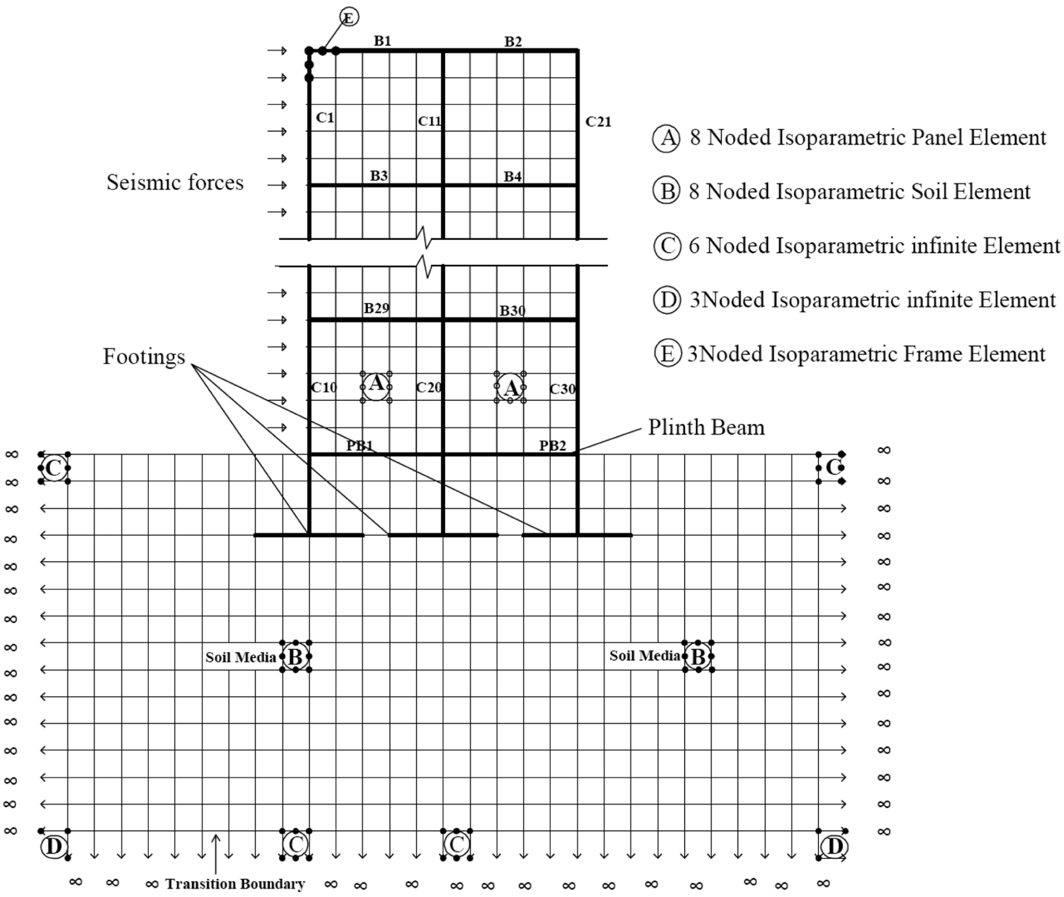

Fig.1 Finite-infinite element idealization of infilled frame-homogeneous soil system

using static method as per IS:1893 (Part I):2002. The parameters used for estimation of seismic forces are provided Table 2 and estimated seismic forces are provided in Table 3.

The nonlinear interaction analysis is carried out using mixed incremental-iterative solution algorithm. The total vertical load of 3960 kN and seismic loads are applied in twelve load increments. Initially, the behaviour of the interaction system is found to be linear elastic up to load value of 30% of the total load (first load increment). Thereafter, the curve becomes nonlinear and, therefore, the remaining load increments are smaller (10, 10, 10, 5, 5, 5, 5, 5, 5, 5 and 5% of total load). The twelfth load increment corresponds to load factor 1.0 (i.e. total load on the structure). The norm of residual force for convergence is considered and a tolerance limit of 1% is selected for residual forces. The interaction behaviour of both interaction systems is studied with respect to differential settlements caused due to incrementally applied loads of the nonlinear analysis. The total load applied corresponds to load factor of unity. The variation of axial force and bending moments in the columns, bending moments in the floor and plinth beams, contact pressure distribution below footings and stresses in the infill panels are investigated due to increase in the differential settlements. A comparison is made between nonlinear interaction behaviour of PF-HS and INF-HS.

Table 1 Geometrical and material properties of the superstructure, infill and soil

S.N.	Structural components	Size and material properties of various components		
1	All floor and plinth beams	0.30 m × 0.40 m		
2	Columns	Floor	Outer	Inner
		I & II	0.30 m × 0.30 m	0.35 m × 0.35 m
		III & IV	0.35 m × 0.35 m	0.40 m × 0.40 m
		V & VI	0.40 m × 0.40 m	0.45 m × 0.45 m
		VII & VIII	0.45 m × 0.45 m	0.50 m × 0.50 m
		IX and X	0.50 m × 0.50 m	0.60 m × 0.60 m
4	All footings	3.0 m × 3.0 m × 1.0 m		
5	Number of bays	2		
6	Number of storeys	10		
7	Bay width	4.5		
8	Modulus of elasticity of concrete	2.1×10^7 kN/m^2		
9	Poisson's ratio of concrete	0.20		
10	Modulus of elasticity of bricks	0.7 x 10^7 kN/m^2		
11	Poisson's ratio of bricks	0.15		
12	Uniformly distributed load on floor beam and plinth beam	40 kN/m		
	Nonlinear soil properties			
13	Initial tangent modulus (E_i)	45000.0 kN/m^2		
14	Poisson's ratio (μ)	0.30		
15	Cohesion (c)	0.0 kN/m^2		
16	Angle of internal friction (Ø)	37.5^0		
17	Modulus number (K)	500.0		
18	Exponent (n)	0.92		
19	Failure ratio (R_f)	0.85		
20	Atmospheric pressure (P_a)	100.0 kN/m^2		

Table 2 Parameters for estimation of seismic forces

Sr. No.	Parameter/Particulars	Value/type
1	Seismic zone	V
2	Seismic intensity	Severe
3	Zone factor	0.36
4	Type of soil	Medium
5	Importance factor	1.0
6	Type of building	Moment resisting frame building with brick infill panel
7	Response reduction factor	5.0

Table 3 Seismic force (kN) at different floor levels

Floor Level	I	II	III	IV	V	VI	VII	VIII	XI	X
Seismic force	0.6	2.5	5.5	9.7	15.0	21.4	28.8	37.2	46.6	37.8

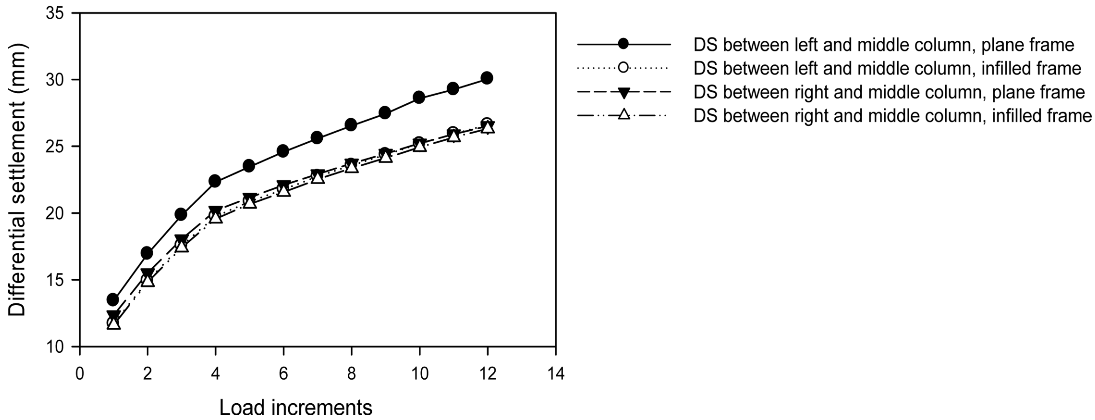

Fig. 2 Variation of differential settlement with load increments

6.2 Variation of differential settlement with load increment

In the present problem, the differential settlement (DS) between left footing and middle footing and between right and middle footing is considered to investigate the structural behaviour of the infilled frame-homogeneous soil system.

Fig. 2 shows the variation of differential settlement with the load increments of NLIA. The differential settlement between left and middle footings varies from 11.71 mm (first load increment) to 26.60 mm (twelfth load increment) and the nature of variation is found to be bilinear. The value of differential settlement for PF-HS varies from 13.44 mm to 30.04 mm. The differential settlement in INF-HS is nearly 13% less than that of PF-HS.

The value of differential settlement between right and middle footings of INF-HS varies from 11.62 mm (first load increment) to 26.32 mm (twelfth load increment) whereas it varies from 12.36 mm to 26.52 mm for PF-HS. The insignificant difference is found in the differential settlement of PF-HS and INF-HS.

6.3 Axial force in the columns

Table 4 shows the value of axial force in the left columns of PF-HS and INF-HS due to NLIA. The infilled frame-homogeneous soil interaction analysis (NLIA-INF) is carried out considering the infill as structural unit taking part in the load resisting system while the plane frame-homogeneous interaction analysis (NLIA-PF) is carried out neglecting the presence of infill. The comparison of axial forces due to NLIA-INF and NLIA-PF reveals that the interaction effect causes redistribution of the forces in the column members. The inclusion of infill causes significant decrease in the axial forces due to significant increase in the stiffness of the system.

A significant decrease of nearly 22 to 75% is found in the left columns of INF-HS. The

Table 4 Axial force (kN) in left columns of frame-homogeneous soil system

Storey Level (1)	Member (2)	NLIA-PF (3)	NLIA-INF (4)	% Diff. (3-4)
X	C_1	104.00	30.05	-71.11
IX	C_2	217.85	59.15	-72.85
VIII	C_3	323.01	80.72	-75.01
VII	C_4	410.25	106.06	-74.15
VI	C_5	496.24	122.72	-75.27
V	C_6	578.44	149.06	-74.23
IV	C_7	670.65	193.23	-71.19
III	C_8	756.37	257.58	-65.95
II	C_9	861.60	401.36	-53.42
I	C_{10}	964.91	751.58	-22.11
Below GL	C_{11}	1116.77	1112.11	-0.42

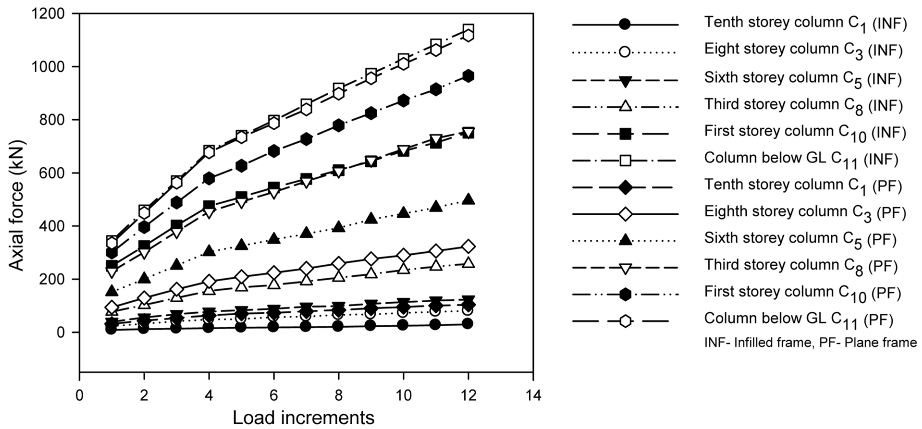

Fig. 3 Variation of axial force in left columns with load increments

maximum decrease of nearly 75% is found in the column of sixth storey whereas minimum decrease of nearly 22% is found in the first storey column. There is insignificant decrease in the axial force of the column below ground level. Fig. 3 shows the variation of axial force with the load increments of NLIA. The axial force increase with increase in load increments and bilinear variation is found for both NLIA-INF as well as NLIA-PF.

Table 5 shows the value of axial force in middle columns of INF-HS and PF-HS due to nonlinear analysis. The comparison of axial force between NLIA-INF and NLIA-PF reveals that the interaction effect causes significant decrease in the axial force of the middle columns of INF-HS due to inclusion of infill.

A significant decrease of nearly 5 to 69% is found in the middle columns of INF-HS. The maximum decrease of nearly 69% is found in the top storey column whereas minimum decrease of nearly 5% is found in the column below ground level.

Fig. 4 shows the variation of axial force in the middle columns with the load increments of NLIA. The axial force increase with increase in load increments and bilinear variation is found for both NLIA-INF and NLIA-PF. Table 6 shows the value of axial force in right columns of INF-HS and PF-HS due to nonlinear analysis. The comparison of axial forces due to NLIA-INF and NLIA-PF

Table 5 Axial force (kN) in middle columns of frame-homogeneous soil system

Storey Level (1)	Member (2)	NLIA-PF (3)	NLIA-INF (4)	% Diff. (3-4)
X	C_{12}	134.22	41.64	-68.98
IX	C_{13}	240.94	85.71	-64.43
VIII	C_{14}	339.55	158.01	-53.46
VII	C_{15}	415.15	186.60	-55.05
VI	C_{16}	489.27	249.30	-49.05
V	C_{17}	565.25	318.40	-43.67
IV	C_{18}	642.65	403.68	-37.19
III	C_{19}	704.78	424.52	-39.77
II	C_{20}	743.63	441.12	-40.68
I	C_{21}	798.64	550.97	-31.01
Below GL	C_{22}	814.29	771.59	-5.24

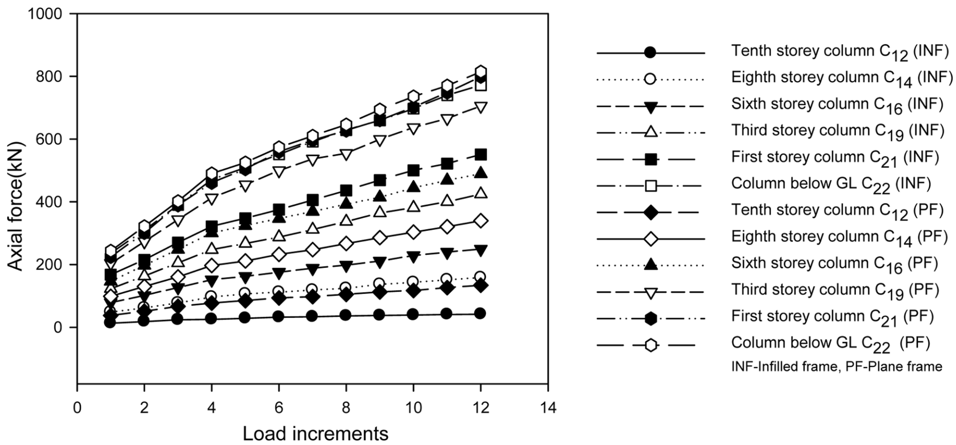

Fig. 4 Variation of axial force in middle columns with load increments

Table 6 Axial force (kN) in right columns of frame-homogeneous soil system

Storey Level (1)	Member (2)	NLIA-PF (3)	NLIA-INF (4)	% Diff. (3-4)
X	C_{23}	124.32	43.53	-64.99
IX	C_{24}	279.68	87.81	-68.60
VIII	C_{25}	445.59	145.37	-67.38
VII	C_{26}	640.23	216.11	-66.24
VI	C_{27}	843.21	311.58	-63.05
V	C_{28}	1021.43	414.41	-59.43
IV	C_{29}	1236.62	518.38	-58.08
III	C_{30}	1456.32	688.62	-52.72
II	C_{31}	1644.38	951.84	-42.12
I	C_{32}	1869.61	1734.51	-7.23
Below GL	C_{33}	1941.33	1908.53	-1.69

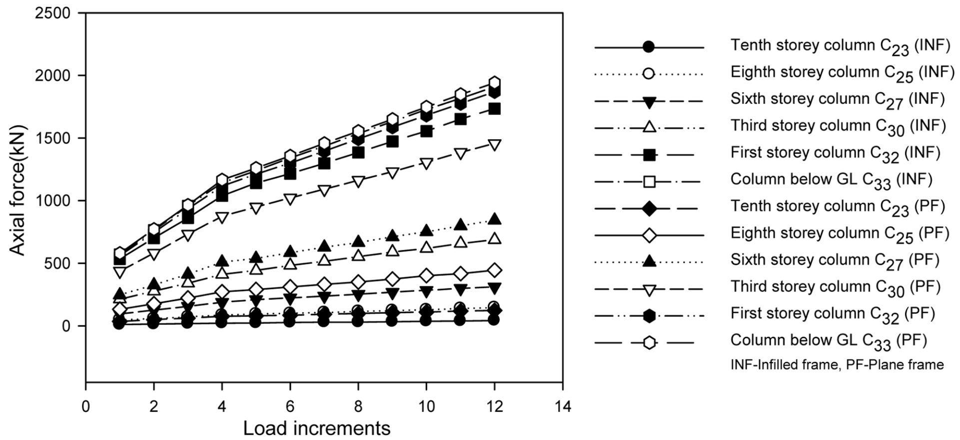

Fig. 5 Variation of axial force in right columns with load increments

reveals that the interaction effect causes significant decrease in the axial force in the right columns due to inclusion of infill.

A significant decrease of nearly 2 to 68% is found in the right columns due to NLIA-INF. The maximum decrease of nearly 68% is found in the ninth storey column whereas minimum decrease of nearly 2% is found in the column below ground level. Fig. 5 shows the variation of axial force in the right columns with the load increments of NLIA. The axial force increase with increase in load increments and bilinear variation is found for both NLIA-INF and NLIA-PF.

6.4 Bending moments in the columns

Table 7 shows the values of bending moment in the left columns of INF-HS and PF-HS. The inclusion of infill causes significant variation in the bending moments of the left columns.

There is highly significant decrease in the values of bending moment which reduces to very low value in case of NLIA-INF. This is because of the tremendous increase in the stiffness of the system due to inclusion of infill. The reversal in the sign of bending moments is found at the top end of the columns of 9th, 7th, 6th, 5th and 3rd storeys and at both ends of column of 2nd storey. The increase of nearly 80% is found at bottom end of first storey column. An insignificant decrease in the bending moment of column below ground level is found as there is no infill below ground level. Fig. 6 shows variation of bending moments in the left columns due to NLIA. The bending moments increase with increase in load increments and bilinear variation is found for both NLIA-INF and NLIA-PF.

Table 8 shows the values of bending moment in the middle columns of INF-HS and PF-HS. The value of bending moment reduces to very low value in case of NLIA-INF for all storeys except the first storey. The insignificant variation is found in the bending moments of the columns of first storey and the column below ground level except at the top end of the first storey column where the reversal in the sign of bending moment occurs. Fig. 7 shows variation of bending moments in the middle columns. The bilinear variation in the bending moments is found due to NLIA-INF as well as NLIA-PF.

Table 9 shows the values of bending moment in the right columns of INF-HS and PF-HS. The value of bending moments in all columns reduces to very low value except at the bottom end of the

Table 7 Bending moments (kN-m) in left columns of frame-homogeneous soil system

Storey Level (1)	Member (2)	NLIA-PF (3)	NLIA-INF (4)	% Diff. (3-4)
X	C_1	-74.59 -65.88	-0.13 -2.25	** **
IX	C_2	-26.30 -29.89	1.03 -1.42	* **
VIII	C_3	-41.45 -44.29	-0.57 -1.98	** **
VII	C_4	-15.50 -17.32	0.72 -2.10	* **
VI	C_5	-33.13 -34.46	0.94 -1.49	* **
V	C_6	-13.41 -12.11	0.92 -1.71	* **
IV	C_7	-36.05 -28.13	-0.24 -2.11	** **
III	C_8	-27.05 -2.35	0.30 -2.42	* 2.98
II	C_9	-74.47 8.54	-3.08 -4.75	* *
I	C_{10}	-132.59 88.62	-5.56 159.57	** 80.06
Below GL	C_{11}	-338.12 -390.63	-296.50 -374.13	-12.31 -4.22

*Reversal in sign, **Very high difference in values.

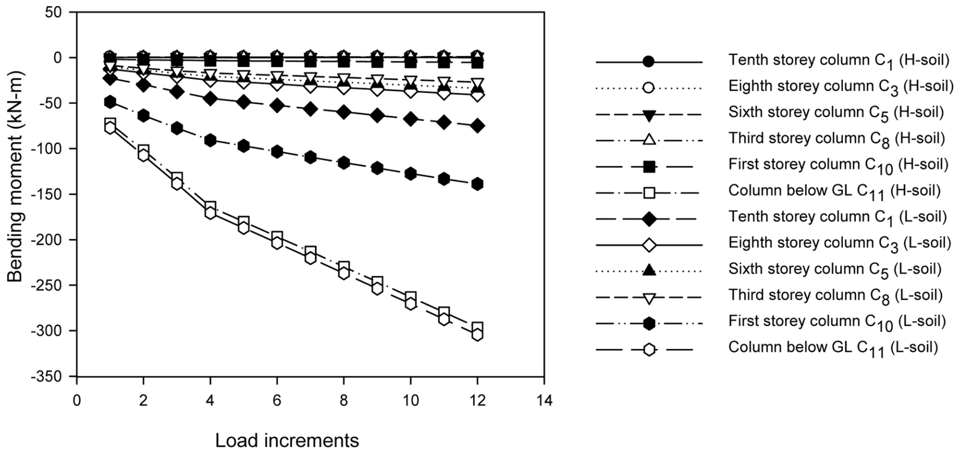

Fig. 6 Variation of bending moment at roof level in left columns with load increments

Table 8 Bending moments (kN-m) in middle columns of frame-homogeneous soil system

Storey Level (1)	Member (2)	NLIA-PF (3)	NLIA-INF (4)	% Diff. (3-4)
X	C_{12}	34.05	0.26	**
		22.43	0.67	**
IX	C_{13}	68.98	0.20	**
		56.05	1.44	**
VIII	C_{14}	97.61	1.12	**
		83.03	1.83	**
VII	C_{15}	117.27	1.08	**
		105.32	1.34	**
VI	C_{16}	132.84	2.29	**
		121.64	3.20	**
V	C_{17}	140.57	1.52	**
		134.82	2.40	**
IV	C_{18}	144.64	2.52	**
		148.68	3.54	**
III	C_{19}	133.36	2.96	**
		157.28	3.08	**
II	C_{20}	96.65	1.40	**
		230.91	3.98	**
I	C_{21}	-50.69	0.39	*
		337.10	242.97	-27.92
Below GL	C_{22}	-384.93	-368.31	-4.32
		0.22	-1.77	*

*Reversal in sign, **Very high difference in values

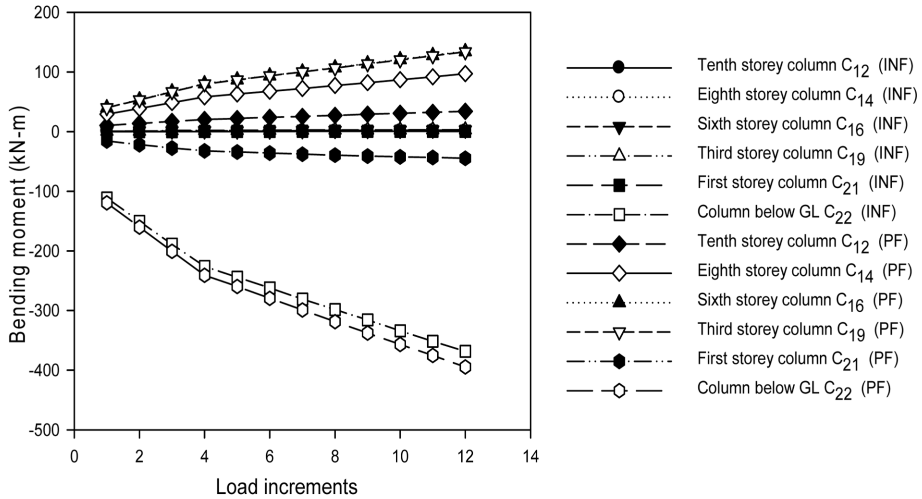

Fig. 7 Variation of bending moment at roof level in middle columns with load increme

Table 9 Bending moments (kN-m) in right columns of frame-homogeneous soil system

Storey Level (1)	Member (2)	NLIA-PF (3)	NLIA-INF (4)	% Diff. (3-4)
X	C_{23}	109.49	0.48	**
		87.54	0.66	**
IX	C_{24}	96.76	0.34	**
		85.71	1.54	**
VIII	C_{25}	142.79	1.20	**
		127.69	2.18	**
VII	C_{26}	137.09	-0.02	*
		124.54	2.69	**
VI	C_{27}	171.07	0.94	**
		157.09	4.14	**
V	C_{28}	160.11	-0.94	*
		151.01	5.37	**
IV	C_{29}	182.67	0.26	**
		177.39	6.00	**
III	C_{30}	163.84	0.43	**
		181.12	8.34	**
II	C_{31}	150.90	2.68	**
		196.87	10.11	**
I	C_{32}	110.76	7.98	**
		294.35	128.10	-56.48
Below GL	C_{33}	-92.86	-77.95	-16.05
		735.15	710.76	-3.32

*Reversal in sign, **Very high difference in values

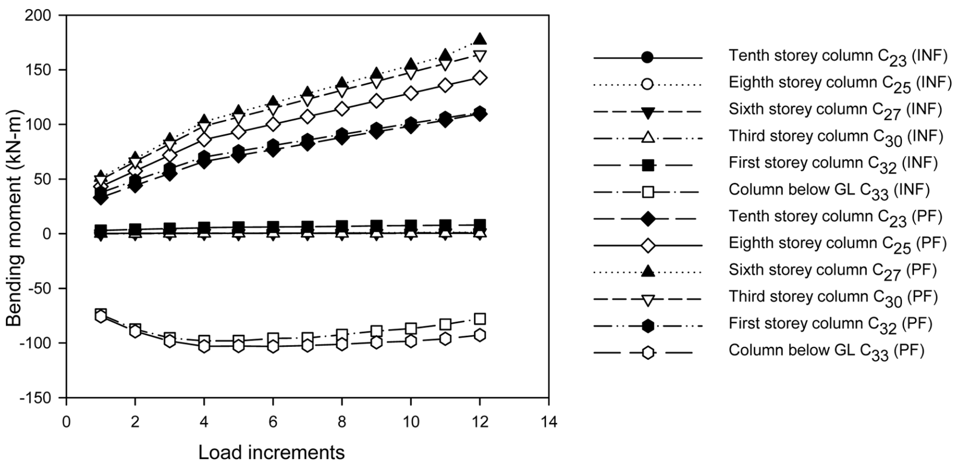

Fig. 8 Variation of bending moment at roof level in right columns with load increments

first storey column where a significant decrease of nearly 56% is found. The insignificant variation takes place in the column below ground level. Fig. 8 shows variation of bending moments in the right columns. The bilinear variation is found for both NLIA-INF and NLIA-PF.

6.5 Bending moments in the floor beams

6.5.1 Bending moment in floor beams of left bay

Table 10 shows the values of bending moment at the inner and outer end of the floor beams of left bay of PF-HS and INF-HS. The highly significant reduction is found in the values of bending moment in case of INF-HS, which become very low. This is because of the tremendous increase in the stiffness of the frame due to inclusion of infill panels, which attract major amount of bending moments. The reversal in the sign of bending moments is found at the outer ends of floor beams of 2nd 5th , and 7th to top storeys. A decrease of nearly 6% is found at the inner end of top storey beam. An increase of nearly 17% is found at the inner end of the first storey beam. A decrease of nearly 43% and 64% is found at the outer and inner ends of the plinth beam respectively. Fig. 9 shows the variation of bending moments in the floor beams of left bay due to NLIA. The bilinear variation is found in the bending moments of floor beams.

Table 10 Bending moments (kN-m) in floor beam of left bay of frame-foundation-soil system

Storey Level (1)	Member (2)	NLIA-PF (3)	NLIA-INF (4)	% Diff. (3-4)
X	B_1	74.18	-1.84	*
		-1.88	-1.76	-6.38
IX	B_3	91.60	-0.63	*
		-7.87	-1.80	**
VIII	B_5	70.83	-0.13	*
		-31.65	-2.92	**
VII	B_7	59.46	-0.02	*
		-48.62	-1.89	**
VI	B_9	50.49	0.25	**
		-61.35	-4.63	**
V	B_{11}	47.10	-0.71	*
		-67.99	-4.05	**
IV	B_{13}	49.01	1.52	**
		-71.24	-7.45	**
III	B_{15}	55.11	0.91	**
		-65.19	-4.71	**
II	B_{17}	76.68	6.26	**
		-49.08	-6.03	**
I	B_{19}	125.96	11.14	**
		-2.56	-3.01	17.58
Plinth level	PB_1	240.99	136.76	-43.25
		122.10	43.30	-64.54

*Reversal in sign, **Very high difference in values

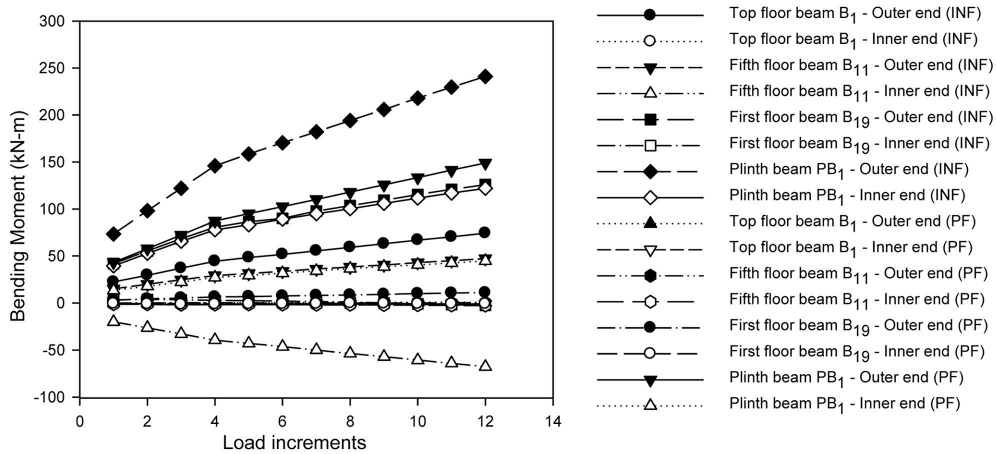

Fig. 9 Variation of bending moment in floor beams of left bay with load increments

Table 11 Bending moments (kN-m) in floor beams of right bay of frame-foundation-soil system

Storey Level (1)	Member (2)	NLIA-PF (3)	NLIA-INF (4)	% Diff. (3-4)
X	B_2	-30.98	0.99	*
		-108.22	-1.28	**
IX	B_4	-82.38	0.40	*
		-184.67	-1.65	**
VIII	B_6	-121.37	1.11	*
		-228.47	-3.05	**
VII	B_8	-151.11	0.33	*
		-264.94	-3.73	**
VI	B_{10}	-176.91	1.25	*
		-296.40	-3.43	**
V	B_{12}	-194.54	0.04	*
		-316.77	-3.87	**
IV	B_{14}	-208.05	0.15	*
		-331.61	-5.97	**
III	B_{16}	-213.59	-2.18	**
		-341.07	-4.76	**
II	B_{18}	-205.66	0.35	*
		-331.76	-11.37	**
I	B_{20}	-176.97	-2.38	**
		-305.29	-16.89	**
Plinth level	PB_2	-74. 49	81.91	*
		-200.35	-51.14	-74.47

*Reversal in sign, **Very high difference in values

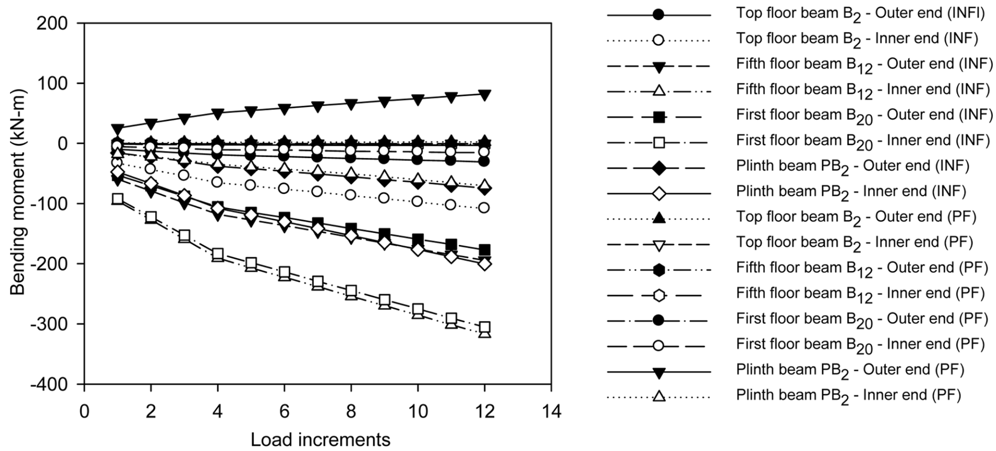

Fig. 10 Variation of bending moment in floor beams of right bay with load increments

6.5.2 Bending moment in floor beams of right bay

Table 11 shows the values of bending moment at the inner and outer end of the floor beams of left bay of PF-HS and INF-HS. The highly significant decrease is found in the values of bending moment, which get reduced to very low value in case of NLIA-INF. The reversal in the sign of bending moments is found at the inner ends of the floor beams of all the storeys except the third storey. A decrease of nearly 74% is found at the outer end of the plinth beam.

Fig. 10 shows the variation of bending moments in the floor beams of right bay due to NLIA. The bilinear variation is found in the bending moments of all the beams.

6.6 Contact pressures below footings

Fig. 11 shows the variation of contact pressure below left footing with various load increments of NLIA-INF and NLIA-PF in the non-dimensional form.

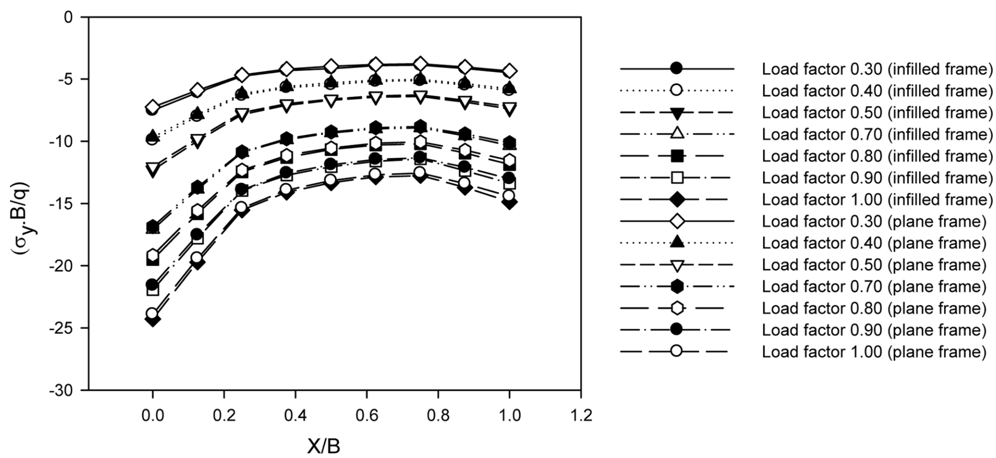

Fig. 11 Variation of contact pressure along length of left footing with load increments

The contact pressure increases with increase in load increments. The comparison of contact pressure below the left footing due to NLIA-INF and NLIA-PF reveals that the variation of contact pressure is found to be almost same for both the interaction systems. The maximum contact pressure is found below the left edge of the footing, whereas it is found to be the minimum below the middle of the footing. The contact pressure below right edge of the footing is nearly 37% less than that below left edge. Fig. 12 shows the variation of contact pressure below middle footing for various load increments of NLIA in the non-dimensional form.

The contact pressures distribution is found to be symmetrical with respect to the centre line of the footing. The variation of contact pressure below the middle footing of INF-HS and PF-HS is found to be almost the same. The contact pressure below the left edge of middle footing is found to be significantly less (nearly 57%) compared to the left edge of left footing. The contact pressure at the left and right edges is nearly 15% more compared to the contact pressure at the middle point of the footing.

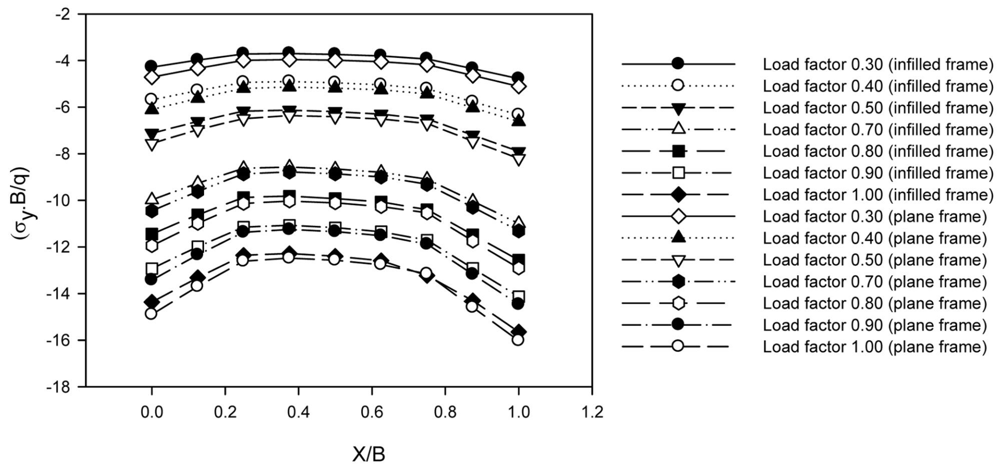

Fig. 12 Variation of contact pressure along length of middle footing with load increments

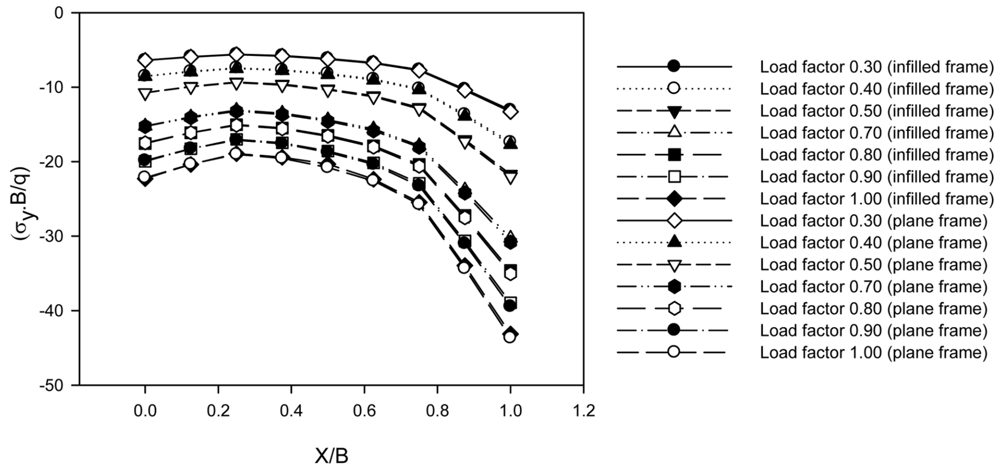

Fig. 13 Variation of contact pressure along length of right footing with load increments

Fig. 13 shows the variation of contact pressure below right footing for various load increments of NLIA in the non-dimensional form. The comparison of contact pressure below the right footing of PF-HS and INF-HS reveals that variation of contact pressure is found to be almost the same. The contract pressure at the left edge of the right footing is found to be nearly 92% less compared to the contact pressure at the right edge. The comparison of contact pressure distribution between left and right footing reveals that the contact pressure at the right edge of the right footing is significantly higher (nearly 67%), whereas a marginal decrease of nearly 7% is found at the left edge of the right footing. The increase of nearly 37% is found at the middle point of the right footing.

6.7 Variation of principal stresses within each infill panel

The stresses in the infill panels are developed mainly due to the interaction between the infill and the bounding frame. There exists an element at each storey infill panel, which carries the maximum principal stress. These elements have been called as highly stressed panel element. The highly stressed panel element at each storey is identified and the maximum principal stress is evaluated. The principal stress is found to be the minimum in the infill panel of the top storey whereas it is found to be the maximum in the infill panel of the first storey. Fig. 14 shows the variation of maximum principal stress in highly stressed panel elements of each storey for various load increments of NLIA. It is found that the maximum principal stress increases with the increase in load increment and varies in bilinear manner. Fig. 15 shows the highly stressed panel element at each storey.

7. Conclusions

(i) The differential settlement between left and middle footings of infilled frame-homogeneous soil system is nearly 13% less than that of plane frame-homogeneous soil system. The insignificant difference is found in differential settlement between right footing and middle footing of both the interaction system.

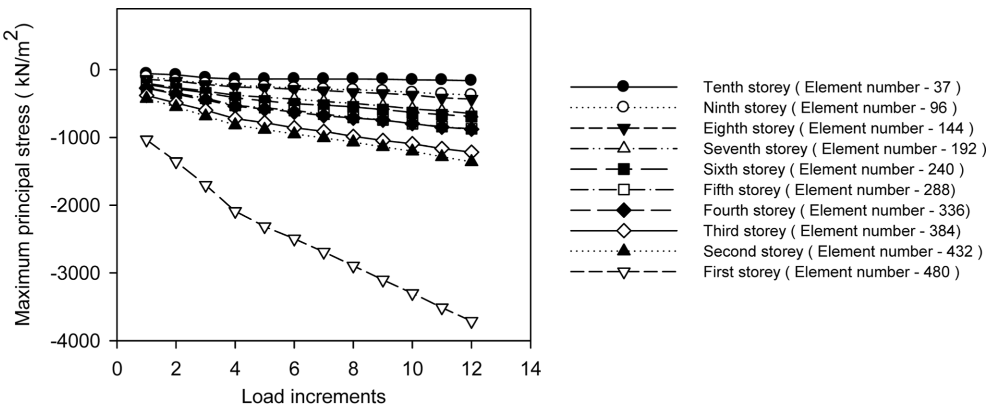

Fig 14 Variation of maximum principal stress in highly stressed elements of infilled frame

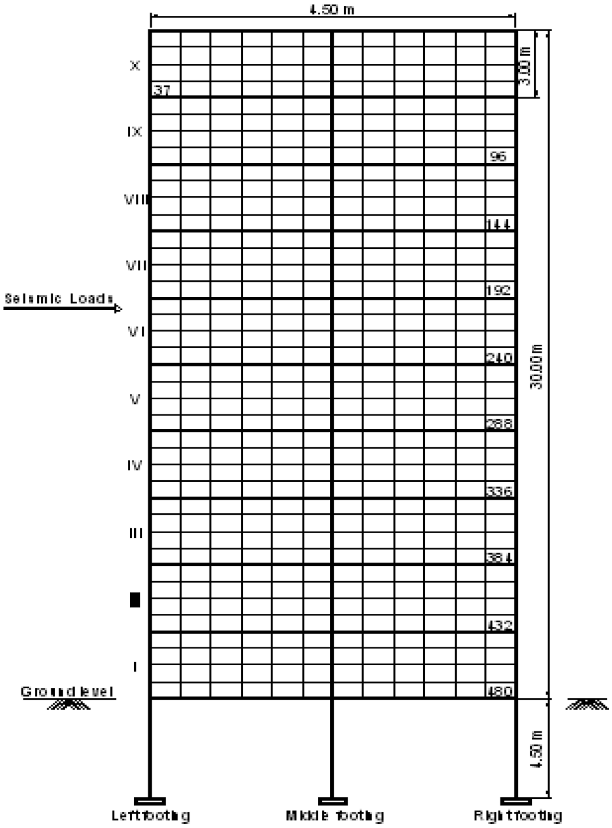

Fig. 15 Location of highly stressed panel element at each storey

(ii) There is significant reduction in the axial force of all the columns due to inclusion of infill walls.
(iii) The bending moment in the columns and beams reduce to very low value because of tremendous increase in the stiffness of the frame due to inclusion of infill panels.
(iv) The nonlinear analysis suggests that differential settlements and forces in the frame members and maximum principal stress in the infill panels vary in bilinear manner.
(v) The contact pressure below all footings increase with increase in the load increments. The maximum contact pressures are found in the right footings which settles more compared to left and middle footings. The contact pressure distribution is found to be symmetrical for the middle footing.

References

Abate, G., Massimino, M.R. and Maugeri, M. (2007), "Soil plasticity and uplifting effects on soil-structure interaction", *Workshop of ETC-12 Evaluation Committee for the Application, Geotechnical Symposium*, Rome, Italy.

Aljanabi, A.I.M., Farid, B.J.M. and Mohamed, A.A.A. (1990), "Interaction of plane frames with elastic

foundation having normal and shear moduli of subgrade reactions", *Int. J. Comput. Struct.*, **36**(6), 1047-1056.
Asteris, P.G. (2003), "Lateral stiffness of brick masonry infilled plane frames", *J. Struct. Eng.,* **129**(8), 1071-1079.
Asteris, P.G. (2008), "Finite element micro modeling of infilled frames", *Electron. J. Struct. Engg.*, **129**(8), 1071-1079.
Asteris, P.G., Antoniou, S.T., Sophianopoulos, D.S. and Chrysostomou, C.Z. (2011), "Mathematical macromodeling of infilled frames: State of the art", *J. Struct. Eng.*, **137**(12), 1508-1517.
Chore, H.S., Ingle, R.K. and Sawant, V.A. (2010), "Building frame-pile foundation-soil interaction analysis: a parametric study", *Interact. Multis. Mech.*, **3**(1), 55-59.
Chrysostomou, C.Z. and Asteris, P.G. (2012). "On the in-plane properties and capacities of infilled frames", *Eng. Struct.*, **41**, 385-402.
Desai, C.S. and Lightner, J.G. (1985), "Mixed finite element procedure for soil-structure interaction and construction sequences", *Int. J. Numer. Meth. Eng.*, **21**, 801-824.
Desai, C.S., Phan, H.V. and Perumpral, J.V. (1982), "Mechanics of three-dimensional soil-structure interaction", *J. Struct. Eng. Div. ASCE*, **108**(5), 1-20.
Duncan, J.M. and Chang, C.Y. (1970), "Nonlinear analysis of stress and strain in soils", *J. SM FE, ASCE,* **96**, 1629-1654.
Fardis, M.N. and Panagiotakos, T.B. (1997), "Seismic design and response of bare and masonry infilled reinforced concrete buildings part II: Infilled structures", *J. Earthq. Eng.*, **1**(3), 475-503.
Hinton, E. and Owen, D.R.J. (1977), *Finite Element Programming*, Academic Press, London.
Hora, M. and Patel, A.N. (2005), "Computational methodology for non-linear soil-structure interaction analysis of infilled building frames", *Proc. Int. Geot. Conf. St. Petersburg,* Vol. **I**, 175-181, Saint Petersburg, May.
Junvi, Y., Feng, J., Xu, Y., Wang, G. and Zhang, C. (2003), "A seismic free input model for FE-SBFE coupling in time domain", *J. Earthq. Eng. Eng. Vib.*, **2**(1), 51-58.
Kaushik, H.B., Rai, D.C. and Jain, S.K. (2006), "Code approaches to seismic design of masonry-infilled reinforced concrete frames: A state-of-the-art review", *Earthq. Spectra*, **22**, 961-983.
Kim, D.K. and Yun, C.B. (2003), "Time domain earthquake response analysis method for 2-D soil-structure interaction systems", *Struct. Eng. Mech.*, **15**(6), 717-733.
Kondner, R.L. and Zelasko, J.S. (1963), "A hyperbolic stress-strain formulation for sands", *Proceedings of Second Pan-American Conf. SM & FE*, Vol. **1**, 289-324, Brazil.
Kumar, P. (1985), "Static infinite element formulation", *J. Struct. Eng. Div. ASCE*, **III**(11), 2355-2375.
Lehman, L. (2004), "An effective finite element approach for soil-structure analysis in time domain", *J. Struct. Eng. Mech*., **21**(4), 437-450.
Mandal, A. (1998), "Soil-structure interaction on building frame: a small scale model study", *Int. J. Struct.*, **18**(2), 92-108.
Manos, G.C., Thaumpta, J. and Yasin, B. (2000), "Influence of masonry infills on the earthquake response of multi-storey reinforced concrete structures", *Proceedings of the 12th World Conference on Earthquake Engineering*, Auckland, New Zealand.
Moghaddam, H.A. (2004), "Lateral load behavior of masonry infilled steel frames with repair and retrofit", *J. Struct. Div., ASCE*, **130**(1), 56-63.
Mohebkhah, A., Tasnimi, A.A. and Moghaddam, H.A. (2008), "Nonlinear analysis of masonry-infilled steel frames with openings using discrete element method", *J. Constr. Steel Res.,* **64**(12), 1463-1472.
Negulescu, C. and Foerster, E. (2010), "Parametric studies and quantitative assessment of the vulnerability of a RC frame building exposed to differential settlements", *Nat. Hazard Earth. Sys.*, **10**, 1781-1792.
Noorzaei, J., Viladkar, M.N. and Godbole, P.N. (1994), "Nonlinear soil-structure interaction in plane frames", *Eng. Comput.*, **11**(4), 303-316.
Puglisi, M., Uzcategui, M. and Florez-Lopez, J. (2009), "Modeling of masonry of infilled frames, Part II: Cracking and damage", *Eng. Struct.*, **31**(1), 119-124.
Puglisi, M., Uzcategui, M. and Florez-Lopez, J. (2009), "Modeling of masonry of infilled frames", Part I: The plastic concentrator", *Eng. Struct.*, **31**(1), 113-118.
Singh, Y. and Das, D. (2006), "Effect of URM infills on seismic performance of RC building frames", *Proceedings of Fourth International Conference on Earthquake Engineering*, Taipei. (Taiwan)

Stavridis, L.T. (2002), "Simplified analysis of layered soil-structure interaction", *J. Struct. Div., ASCE*, **128**(2), 224-230.

Viladkar, M.N., Godbole, P.N. and Noorzaei, J. (1991), "Soil-structure interaction in plane frames using coupled finite-infinite elements", *Int. J. Comput. Struct.*, **39**(5), 535-546.

Viladkar, M.N., Noorzaei, J. and Godbole, P.N. (1994), "Behaviour of infinite elements in an elasto-plastic domain", *Int. J. Comput. Struct.*, **51**(4), 337-342.

Yousuf, M.D. and Bagchi, A. (2010), "Seismic performance of a 20-story steel-frame building in Canada", *Struct. Des. Tall Spec. Build.*, **19**(8), 901-921.